

# 적응 자동 재폐로 및 고장거리 산정을 위한 새로운 1단자 알고리즘

論 文

53A-8-3

## A New One Terminal Numerical Algorithm for Adaptive Autoreclosure and Fault Distance Calculation

조란 라도예비치\* · 愼重麟\*\*  
(Zoran Radojević · Joong-Rin Shin)

**Abstract** - This paper presents a new numerical spectral domain algorithm devoted to blocking unsuccessful automatic reclosing onto permanent faults and fault distance calculation. Arc voltage amplitude and fault distance are calculated from the fundamental and third harmonics of the terminal voltages and currents phasors. From the calculated arc voltage amplitude it can be concluded if the fault is transient arcing fault or permanent arcless fault. If the fault is permanent automatic reclosure should be blocked. The algorithm can be applied for adaptive autoreclosure, distance protection, and fault location. The results of algorithm testing through computer simulation and real field record are given.

**Key Words** : Numerical algorithms, Protection, Fault location, Arc resistance, Transmission lines, Electric power systems, Spectral analysis.

### 1. Introduction

The problem of blocking automatic reclosing on permanent faults is investigated in the last decade. It is known that somewhat about 80% to as high as 90% of faults on most lines are transient. For such faults the service can be restored by automatically reclosing the power circuit breaker. This can improve power system transient stability and reliability providing much higher service continuity to the customers. However, reclosure onto a permanent fault may aggravate the potential damage to the system and equipment. For some extra-high-voltage lines, especially near generating plants, the classical automatic reclosing of breakers cannot be used.

New numerical protection algorithms gave an opportunity to control the automating reclosing from a substation computer. Main problem to be solved is to make distinction between permanent and transient faults. Some interesting concepts were proposed in the past. Most of them were based on the analysis of voltage on the opened phase conductor during the reclosing dead time [1-2]. The newly developed algorithms [3-5] were derived by processing line terminal voltage and current during the fault, in other words before the breaker was opened.

In order to improve the quality of power delivery,

digital devices with the fault location algorithms are developed and proposed in the open literature. Distance relays calculate the fault distance in real-time, while the fault location programs are executed after the fault using stored fault data. The rapid progress in microprocessor technology gives us a hope that some numerical algorithms devoted to fault location will be used as algorithms for distance protection, particularly the so called "one terminal fault location algorithms", which use only data measured at relay place [6].

In this paper a new numerical spectral domain algorithm for arcing faults recognition and fault distance calculation using Discrete Fourier Technique will be given.

### 2. Basic Characteristics of a Long Electric Arc

The long electric arc in free air is a plasma discharge, where the plasma allows a current to flow through a gaseous medium. The current can range from a few amps up to thousands of amps.

The nonlinear variations of the arc causes the arc voltage waveform distortion, distorting it into a near square wave with arc voltage amplitude  $V_a$  [7], what is given in Fig. 1. From the Fig. 1 it is obvious that the sign of the arc voltage wave  $v_a$  is the same as sign of the arc current  $i_a$ .

The arc voltage could be modeled by a nonlinear arc resistance [8], or by the piecewise arc voltage-current characteristics [9]. In this paper a new approach is chosen. The arc voltage wave shape is defined numerically on the

\* 正會員 : 建國大學 工大 電氣工學科

\*\* 正會員 : 建國大學 工大 電氣工學科 教授 · 工博

接受日字 : 2004年 3月 12日

最終完了 : 2004年 6月 16日

basis of a great number of arc voltage records obtained in the high voltage laboratory using a transient recorder with the sampling frequency of 10.417 kHz [7].

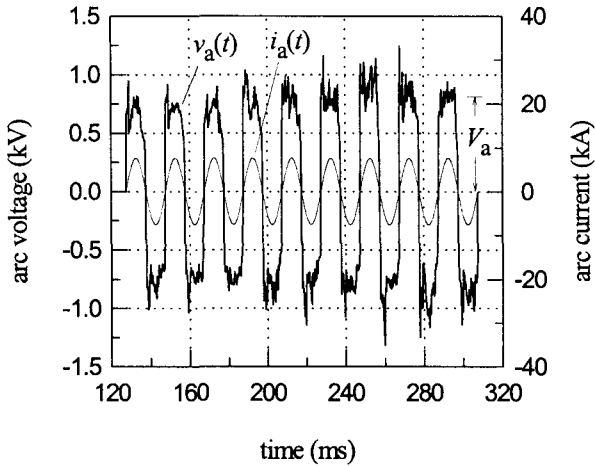


Fig. 1 Real arc voltage and current waveforms

The arc voltage model presented in Fig. 2 is accepted. Fig. 2 gives a normalized cycle of the arc voltage model with arc voltage amplitude  $V_a = 1$  p.u. It is assumed that the sign of these values is determined by the sign of arc current.

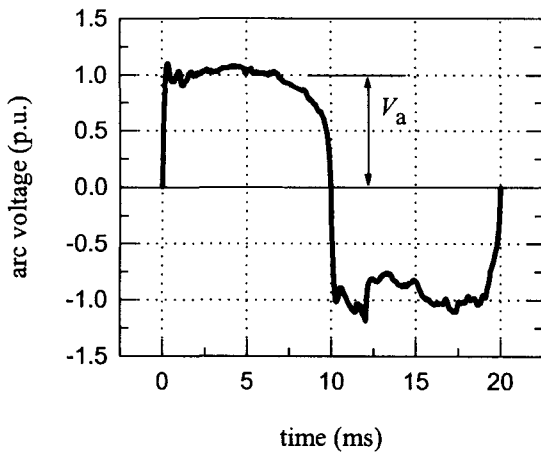


Fig. 2 Typical accepted arc voltage wave shape

The arc model given in Fig. 2 has an important feature: it can be represented by Fourier series containing odd sine components only, as follows:

$$v_a(t) = \sum_{h=1}^{\infty} k_h V_a \sin(h\omega t) \quad (1)$$

where  $h = 1, 3, 5, 7, \dots$  is the harmonic order,  $\omega$  is the fundamental radian frequency and  $k_h$  is the coefficient of the  $h$ -th harmonic.

Using the DFT algorithm it is easy to obtain coefficients  $k_h$  for accepted arc voltage model. These coefficients are given in Table 1.

Table 1. Coefficients of the  $h$  th harmonics of the arc voltage

$h$	1	3	5	7
$k_h$	1.23	0.393	0.213	0.135

In comparison to the other models, the advantage of the arc voltage presentation through the sequence of numerical values is its flexibility. One can create various waveform shapes and calculate the corresponding coefficients  $k_h$ , depending on the modeling application.

### 3. The Fault Model

Let us consider the most frequent single-phase to ground fault on a transmission line fed from both line terminals. The fault model will be given by relation between faulted phase voltage, fault current and earth return path parameters.

Fault voltage may be selected to be zero for a pure metallic fault. Such cases occur, but relatively seldom. The former model may be improved by including into it the fault resistance. The fault resistance originates from the resistance of the arc and resistance of tower footing and ground. In this paper a new accurate model with all important features of arc taken into account is developed. The current path for ground faults adopted in this model includes the arc voltage and the fault resistance.

Fault phase voltage  $v_F$  can be given in time domain, what is depicted in Fig. 3.a), by next relation:

$$v_F(t) = v_a(t) + R_F i_F(t) \quad (2)$$

where  $v_a$  is arc voltage,  $R_F$  is fault resistance and  $i_F$  is fault (arc) current.

New spectral domain fault model, developed in this paper, is depicted in Fig. 3.b). From this picture the  $h$ -th harmonic of the fault voltage can be expressed by next relation:

$$\underline{V}_{Fh} = \underline{V}_{ah} + R_F \underline{I}_{Fh} \quad (3)$$

where  $\underline{V}_{ah}$  is  $h$  th harmonic of the arc voltage and  $\underline{I}_{Fh}$  is  $h$ -th harmonic of the fault (arc) current.

In this paper only fundamental and third harmonic fault model will be used for algorithm developing.

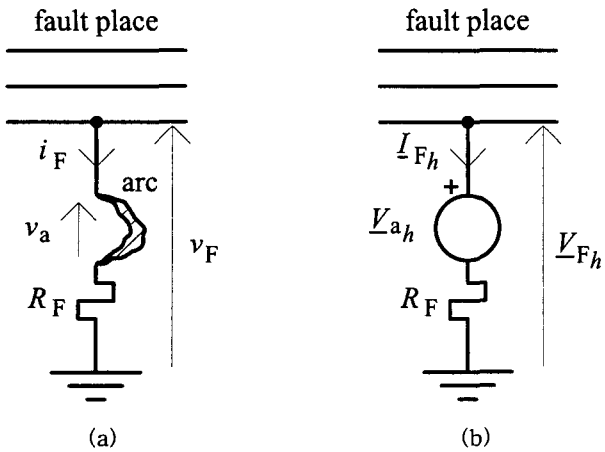


Fig. 3 Fault model given (a) in time domain and (b) in spectral domain for  $h$  th harmonic

It is possible to express the amplitude of the  $h$ -th harmonic of the arc voltage by the next relation:

$$V_{ah} = k_h V_a \tag{4}$$

where  $V_{ah}$  is the amplitude of the  $h$ -th harmonic of the arc voltage.

From(4) it follows:

$$V_{a1} = k_1 V_a = 1.23 V_a \text{ and } V_{a3} = k_3 V_a = 0.393 V_a \tag{5}$$

The arc voltage wave is in phase with the fault arc current, as shown in Fig. 1. That means that the phase of the first harmonic of the arc voltage has to be the same as the phase of the first arc current harmonic, i.e. fault current. The phase of the third harmonic of the arc voltage has to be three times greater than the phase of the first harmonic of arc current. The former observation could be expressed as:

$$\underline{V}_{a1} = k_1 V_a \text{ and } \underline{V}_{a3} = k_3 V_a \tag{6}$$

where  $\underline{V}_{a1}$  and  $\underline{V}_{a3}$  are vectors of the first and the third harmonics of the arc voltage,  $k_1 = k_1 \angle \phi$  and  $k_3 = k_3 \angle 3\phi$  where  $\phi$  is the phase of the first harmonic of the fault current ( $\underline{I}_{F1} = I_{F1} \angle \phi$ ).

#### 4. Arc Voltage Amplitude and Fault Distance Calculation

It is practically impossible to measure the arc voltage, since the fault has an arbitrary location on the line. The idea of this paper is the calculation of the arc voltage

amplitude from the line terminal voltage and current signals obtainable as uniformly digitized quantities at one of the line terminals. The voltages and currents at the line terminals contain harmonics. The distortion of waves depends on the fault distance and the arc voltage amplitude. It could be concluded through spectral analysis that the line terminal voltage and the current contain the harmonics induced by arc voltage, particularly the odd components. These amplitudes are not comparable to the fundamental harmonic amplitude, but in spite of that are recognizable and measurable.

Thus, one of the obvious ways in which arc voltage harmonics could be calculated is to analyze the circuit depicted in Fig.4. In this circuit all variables have radian frequency  $h\omega$  and all the line parameters are calculated in terms of  $h\omega$ . Index  $h$  denotes order of the harmonic.

Let us assume a single phase to ground arcing fault occurring on a three phase overhead line depicted in Fig.4. In Fig.4,  $V_h$  is the  $h$ -th harmonic of the left line terminal phase voltage,  $I_h$  is the  $h$ -th harmonic of the left line terminal current,  $V_{ah}$  is the  $h$ -th harmonic of the arc voltage,  $R_F$  is fault resistance and  $V_{Fh}$  is the  $h$ -th harmonic of the faulted phase voltage on the fault place.

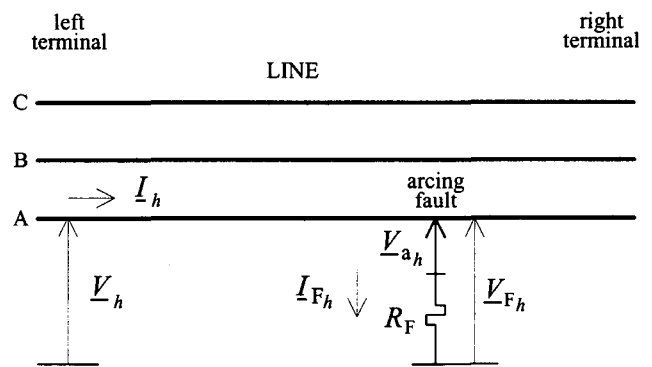


Fig. 4 Single phase to ground arcing fault on three phase power line

The three phase circuit from Fig.4 can be presented by three single phase equivalent circuits: positive (p), negative (n) and zero sequence (0) equivalent circuits. Positive and negative sequence equivalent circuits are equal and are depicted in Fig.5. In Fig. 5,  $z_h$  is positive or negative sequence line impedance. The zero sequence equivalent line circuit is depicted in Fig.6. In Fig.6 all variables and parameters are zero sequence variables and parameters.

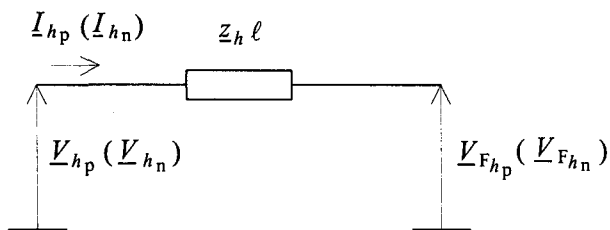


Fig. 5 Positive and negative sequence line equivalent circuit

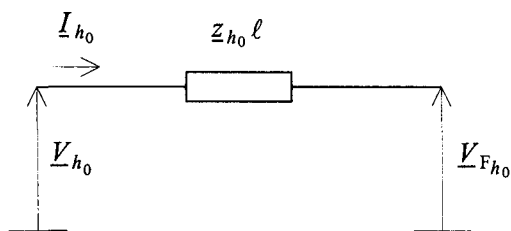


Fig. 6 Zero sequence line equivalent circuit

For the equivalent circuits depicted in Figs.5 and 6 the following equations can be written:

$$\underline{V}_{h_p} = \underline{z}_h \ell \underline{I}_{h_p} + \underline{V}_{Fh_p} \quad (7)$$

$$\underline{V}_{h_n} = \underline{z}_h \ell \underline{I}_{h_n} + \underline{V}_{Fh_n} \quad (8)$$

$$\underline{V}_{h_0} = \underline{z}_h \ell \underline{I}_{h_0} + \underline{V}_{Fh_0} \quad (9)$$

By adding equations (7), (8) and (9), and using basic symmetrical components equations

$$\underline{V}_h = \underline{V}_{h_p} + \underline{V}_{h_n} + \underline{V}_{h_0}$$

and

$$\underline{V}_{Fh} = \underline{V}_{Fh_p} + \underline{V}_{Fh_n} + \underline{V}_{Fh_0}$$

one obtains:

$$\underline{V}_h = \underline{z}_h (\underline{I}_h + \underline{k}_{zh} \underline{I}_{h0}) \ell + \underline{V}_{Fh} \quad (10)$$

where:  $\underline{k}_{zh} = (\underline{z}_{0h} - \underline{z}_h) / \underline{z}_h$  is the zero sequence compensation factor, which can be calculated in advance.

Substituting fault model equation (3) in (10), and using relations (6), next faulted loop equations for fundamental and 3-rd harmonic are obtained:

$$\underline{V}_1 = \underline{z}_1 (\underline{I}_1 + \underline{k}_{z1} \underline{I}_{10}) \ell + \underline{k}_1 \underline{V}_a + R_F \underline{I}_{F1} \quad (11)$$

$$\underline{V}_3 = \underline{z}_3 (\underline{I}_3 + \underline{k}_{z3} \underline{I}_{30}) \ell + \underline{k}_3 \underline{V}_a + R_F \underline{I}_{F3} \quad (12)$$

The fundamental and 3-rd harmonic of the faulted phase voltage and faulted phase current are measured at the relay place, and they are considered as known algorithm input data. But, the fundamental and 3-rd harmonic of the fault current are not measurable at the

relay place. Because of that, the above system of two simultaneous complex equations, (11) and (12), with three unknown variables,  $\underline{V}_a$  and  $R_F$ , can not be solved.

Fortunately, if the fault current is not known, the fault location and arc voltage amplitude can still be accurately calculated using the assumption that the current distribution factors for the parts of the zero sequence network, located on either side of the fault point, have the same arguments [10]. With this simplification, current at the fault location can be expressed in terms of measured faulted phase current, and equations (11) and (12) can be approximately solved.

Because the zero-sequence network is passive we can assume that zero sequence currents supplied from the local and remote systems are in phase. Then fundamental and 3-rd harmonics of fault current can be expressed as:

$$\underline{I}_{F1} = 3 \underline{I}_{F10} = 3 c_{F1} \underline{I}_{10} \quad (13)$$

$$\underline{I}_{F3} = 3 \underline{I}_{F30} = 3 c_{F3} \underline{I}_{30} \quad (14)$$

where  $c_{F1}$  and  $c_{F3}$  are real proportional coefficients. In case in which only arc voltage amplitude and fault distance are to be calculated, the value of  $c_{F1}$  and  $c_{F3}$  are not necessary to be known in advance.

Using above assumption, equation (11) and (12) get the form:

$$\underline{V}_1 = \underline{z}_1 (\underline{I}_1 + \underline{k}_{z1} \underline{I}_{10}) \ell + \underline{k}_1 \underline{V}_a + 3 R_{Fe1} \underline{I}_{10} \quad (15)$$

$$\underline{V}_3 = \underline{z}_3 (\underline{I}_3 + \underline{k}_{z3} \underline{I}_{30}) \ell + \underline{k}_3 \underline{V}_a + 3 R_{Fe3} \underline{I}_{30} \quad (16)$$

where  $R_{Fe1} = c_{F1} R_F$  and  $R_{Fe3} = c_{F3} R_F$ .

Complex equations (15) and (16) give system of four scalar equations:

$$\text{Re}\{\underline{z}_1 (\underline{I}_1 + \underline{k}_{z1} \underline{I}_{10})\} \ell + \text{Re}\{\underline{k}_1\} \underline{V}_a + 3 \text{Re}\{\underline{I}_{10}\} R_{Fe1} = \text{Re}\{\underline{V}_1\} \quad (17)$$

$$\text{Im}\{\underline{z}_1 (\underline{I}_1 + \underline{k}_{z1} \underline{I}_{10})\} \ell + \text{Im}\{\underline{k}_1\} \underline{V}_a + 3 \text{Im}\{\underline{I}_{10}\} R_{Fe1} = \text{Im}\{\underline{V}_1\} \quad (18)$$

$$\text{Re}\{\underline{z}_3 (\underline{I}_3 + \underline{k}_{z3} \underline{I}_{30})\} \ell + \text{Re}\{\underline{k}_3\} \underline{V}_a + 3 \text{Re}\{\underline{I}_{30}\} R_{Fe3} = \text{Re}\{\underline{V}_3\} \quad (19)$$

$$\text{Im}\{\underline{z}_3 (\underline{I}_3 + \underline{k}_{z3} \underline{I}_{30})\} \ell + \text{Im}\{\underline{k}_3\} \underline{V}_a + 3 \text{Im}\{\underline{I}_{30}\} R_{Fe3} = \text{Im}\{\underline{V}_3\} \quad (20)$$

from which unknown arc voltage amplitude and fault distance can be calculated.

### 5. Fault Type Detection

The faults encountered on the transmission lines can be classified as transient or permanent faults [11]. In the case of transient fault reclosing is successful and desirable. If the fault is permanent, reclosing is not desirable, and an algorithm should be able to block automatic reclosing and locks out reclosing onto permanent fault.

Transient faults are faults, such as insulator flashovers, that are quickly cleared by switching the line and do not recur if the line is quickly reclosed. The most common cause of this type of fault is lightning. Transient faults are followed by a long electric arc, whose length is longer than the flashover length of the suspension insulator string. Permanent faults are faults that do not clear themselves, but that must be repaired, such as a broken conductor. Permanent faults are not followed by an electric arc. They are arcless faults.

Because it is practically impossible to measure the arc voltage, since the fault has an arbitrary location on the line, an algorithm will distinguish transient from permanent fault, using calculated value of the arc voltage amplitude.

After calculating arc voltage amplitude algorithm can make decision whether the fault is with arc (transient fault), or without arc (permanent fault). Fault is transient if calculated value of arc voltage amplitude is greater than product of arc voltage gradient and the length of the arc path, which is equal or greater than the flashover length of a suspension insulator string. The average arc voltage gradient lies between 12 and 15 V/cm [12].

The criterion which can be used for fault type detection is expressed by the following relation:

$$V_{ac} \geq E_a \times L_f \tag{21}$$

where  $V_{ac}$  is calculated arc voltage amplitude,  $E_a$  is average arc voltage gradient, and  $L_f$  is the flashover length of a suspension string. If relation (21) is satisfied, the fault is transient. Otherwise, the fault is permanent.

### 6. Computer Simulated Tests

The tests have been done using the Electromagnetic Transient Program (EMTP) [13]. The schematic diagram of the 400 kV power system on which the tests are based is shown in Fig. 7. Here  $v(t)$  and  $i(t)$  are digitized voltages and currents, and  $D$  is the line length. The line parameters, calculated via line constants program were  $D = 100$  km,  $r = 0.0352\Omega/\text{km}$ ,  $x = 0.3\Omega/\text{km}$ ,  $r_0 = 0.0975\Omega/\text{km}$  and  $x_0 = 0.9\Omega/\text{km}$ . Data for network A

were :  $R_A = 1\Omega$ ,  $L_A = 0.064\text{H}$ ,  $R_{A0} = 2\Omega$  and  $L_{A0} = 0.128\text{H}$ . Data for network B were :  $R_B = 0.5\Omega$ ,  $L_B = 0.032\text{H}$ ,  $R_{B0} = 1\Omega$  and  $L_{B0} = 0.064\text{H}$ . The equivalent electromotive forces of networks A and B were  $E_A = 400\text{kV}$  and  $E_B = 395\text{kV}$ , respectively. The phase angle between them was 20 degrees.

Single-phase to ground faults are simulated at different points on the transmission line. The pre-fault load was present on the line. The left line terminal voltages and currents are sampled with the sampling frequency  $f_s = 6400$  Hz. The duration of data window was  $T_{du} = 20\text{ms}$ .

The arc voltage used by EMTP is assumed to be of square wave shape with amplitude of  $V_a = 5.4$  kV, corrupted by the random noise. A typical waveforms of arc voltage obtained through computer simulation are depicted in Fig. 8, where the instant of the fault inception was 23 ms. Fault resistance were  $R_F = 2\Omega$ .

Impute phase voltage and line currents, measurable at relay place, calculated by EMTP for selected study case are plotted in Figs. 9 and 10, respectively.

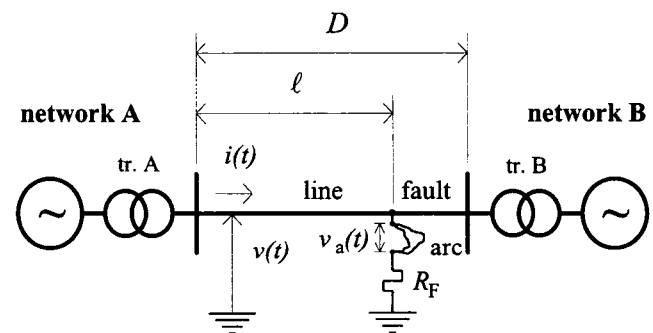


Fig. 7 Test power system

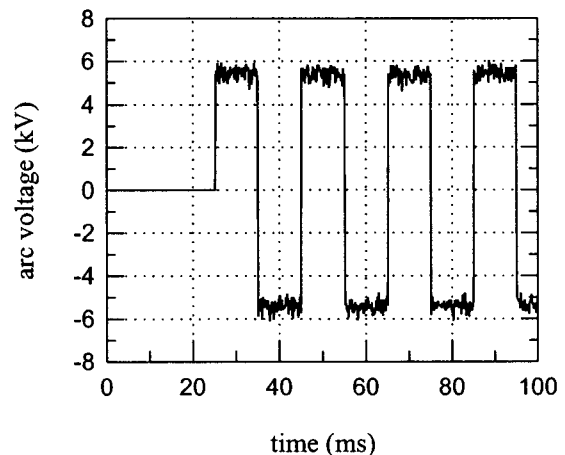


Fig. 8 Arc voltage shape used by EMTP

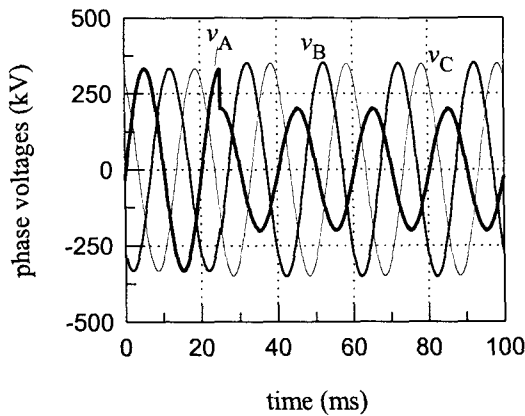


Fig. 9 Distorted input voltages generated by EMTF

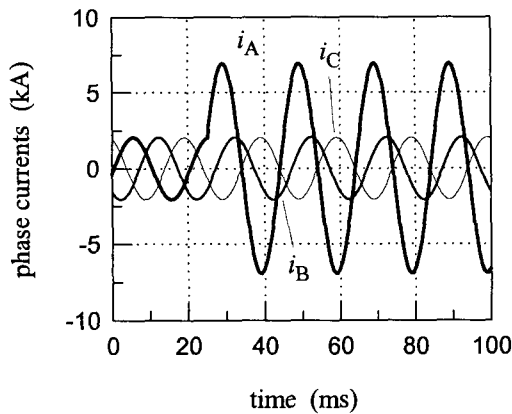


Fig. 10 Distorted input currents generated by EMTF

The fault distance and voltage calculated by algorithm are depicted in fig. 11. The exact unknown model parameters  $l = 60$  km and  $V_a = 5.4$  kV) are obtained fast, after 20 ms, and accurate. From the algorithm speed and accuracy point of view, the results obtained confirm that the algorithm is useful for the application to real overhead lines protection.

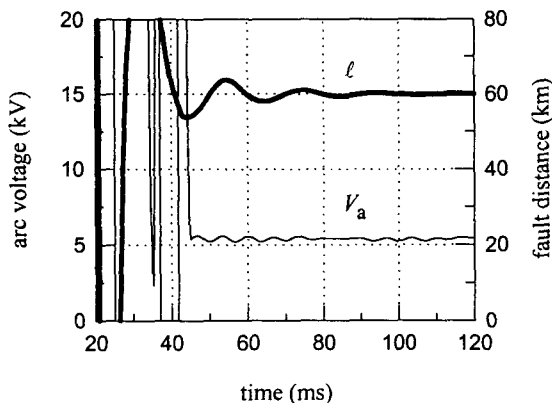


Fig. 11 Calculated fault distance (exact value used by EMTF was 60 km) and arc voltage amplitude (exact value used by EMTF was 5.4 kV)

In order to evaluate the algorithm accuracy the most important fault conditions, such as fault distance and fault resistance, are varied in numerous computer simulations. Those simulations are carried out taking six fault locations, 10, 20, 50, 80, 90 and 100 km, and five fault resistance values, 2, 4, 8, 20 and  $80\Omega$ .

The fault location error, in percentage terms, is calculated using the following equation:

$$e[\%] = \left| \frac{l_c - l_a}{D} \right| \times 100 \quad (22)$$

where  $l_c$  and  $l_a$  represent the calculated fault location and actual location, respectively, and  $D$  denotes the whole line length.

The results of the calculations for various cases that have been studied are presented in Table 2. In most of the cases the fault distance errors are smaller than a typical line span. It could be concluded that the algorithm presented shows enough accuracy for a real application.

Table 2. The fault location error [%] for various values of actual fault distance and fault resistance

Fault resistance $R_F[\Omega]$	Actual fault distance $l[km]$					
	10	20	50	80	90	100
2	0.01	0.01	0.03	0.01	0.38	0.87
4	0.07	0.04	0.01	0.33	0.56	1.51
8	0.10	0.14	0.01	0.51	1.06	2.50
20	0.29	0.28	0.03	0.99	2.18	5.01
80	1.05	0.91	0.37	2.09	4.60	9.95

In order to check the validity of the algorithm presented, voltages and currents, recorded during faults on a 110 kV network, are processed. Here, a typical example of an arcing fault will be demonstrated. In Figs. 12 and 13 voltages and currents measured by the relay before and during a single-phase line to ground fault over arc are respectively presented. All signals are sampled with the sampling frequency  $f_s = 1600$  Hz. The duration of data window was  $T_{du} = 20$  ms.

After data processing, the results of the application of the algorithm presented are depicted in Fig. 14. The exact fault location (see Fig. 14)  $l = 12.8$  km was calculated. Additionally, it is determined that the fault was over an arc with the calculated amplitude plotted in Fig. 14. As it can be observed, the arc voltage amplitude was approximately 2 kV.

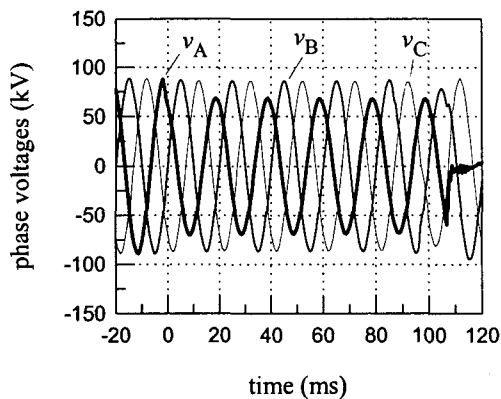


Fig. 12 Input voltages measured by the relay

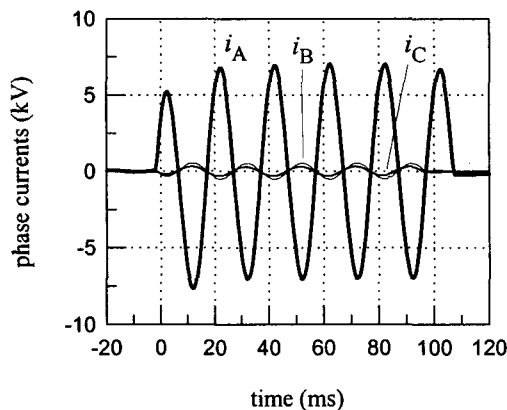


Fig. 13 Input currents measured by the relay

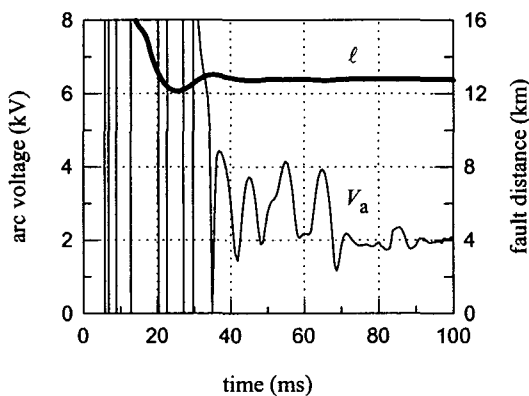


Fig. 14 Calculated arc voltage amplitude and fault distance

Because the minimal length of the arc path determined by the arcing horns distance was 0.85 m, minimal arc voltage amplitude expected was 1.1 kV, obtained as a product of the minimal arc length and the electric field inside the arc, which is practically constant along the arc and has the average value of 1.3 kV/m. The calculated arc voltage amplitude indicates that the arc was prolonged

with regard to its minimal length, equal to the distance between arcing horns.

Comparing calculated arc voltage amplitude of 2 kV with its expected minimally possible value of 1.1 kV, can be concluded that the fault is transient and that reclosing will be successful.

By the inspection of the fault analyzed, it was concluded that the estimated distance was the exact one.

## 8. Conclusion

A new numerical algorithm for arcing faults recognition and for fault distance calculation is developed. The algorithm is derived by processing line terminal voltages and currents during the period between the fault inception and fault clearance. It is based on the spectral analysis of the input phase voltages and line currents signals measured by numerical relay. Only fundamental and third harmonic phasors calculated by Discrete Fourier Technique are needed for algorithm development.

The arc voltage amplitude calculated in algorithm can be used for blocking reclosing of transmissions lines with permanent faults, whereas the fault distance calculated in algorithm can be used for distance protection or for fault location.

A new spectral domain fault model with all significant arc features included is given.

The algorithm was successfully tested with data obtained through computer simulation and data recorded in the real power system.

## References

- [1] R. K. Aggarwal, A. T. Johns, Y. H. Song, R. W. Dunn and D. S. Fitton, "Neural-network based adaptive single-pole autoreclosure technique for EHV transmission systems," IEE Proc.-Gener. Transm. Distrib., vol. 141, pp. 155-160, March 1994.
- [2] Y. Ge, F. Sui and Y. Xiao, "Prediction methods for preventing single-phase reclosing on permanent fault," IEEE Trans. on Power Delivery, vol. 4, pp.114-121, Jan. 1989.
- [3] Z. Radojević, V. Terzija and M. Đurić, "Spectral Domain Arcing Faults Recognition and Fault Distance Calculation in Transmission Systems," Electric Power Systems Research, vol. 37, pp. 105-113, 1996.
- [4] Z. Radojević and M. Đurić, "Arcing Faults Detection and Fault Distance Calculation on Transmission Lines Using Least Square Technique," International Journal of Power and Energy Systems, vol. 18, no. 3, pp.176-181, 1998.
- [5] Z. Radojević and Joong-Rin Shin, "Numerical Algorithm for Adaptive Autoreclosure and Fault Distance Calcula-

tion", Proceedings of the KIEE PES Autumn Annual Conference 2003, Mrina Resort, Chungmu, Kuyngsangdo, Korea, November 13-15, 2003, pp. 79-81.

- [6] M. S. Sachdev (Coordinator), "Advancements in Microprocessor Based Protection and Communication," IEEE Tutorial Course Text, Publication No. 97TP120-0, 1997.
- [7] V. Terzija and D. Nelles, "Parametrische Modelle des Lichtbogens und Parameterschätzung auf Grund der simulierten und echten Daten," TB-183/93, Univ. Kaiserslautern, July 1993.
- [8] T. Funabashi, H. Otaguro, Y. Mizuma, L. Dubé, M. Kizilcay and A. Ametani, "Influence of Fault Arc Characteristics on the Accuracy of Digital Fault Locators," IEEE Trans. on Power Delivery, vol. 16, pp. 195-199, April 2001.
- [9] A. T. Johns, R. K. Aggarwal and Y. H. Song, "Improved technique for modelling fault arc on faulted EHV transmission systems," IEE Proc.-Gener. Transm. Distrib., vol. 141, pp. 148-154, March 1994.
- [10] L. Eriksson, M. Saha, G. D. Rockefeller, "An Accurate Fault Locator with Compensation for Apparent Reactance in the Fault Resistance Resulting from Remote-End Infeed," IEEE Trans. on PAS, vol. PAS 104, pp.424-436, February 1985.
- [11] Westinghouse Relay-Instrument Division, Applied Protective Relaying, Westinghouse Electric Corporation, Newark, New York, 1976.
- [12] A. S. Maikapar, "Extinction of an Open Electric Arc," Elektrichestvo, vol. 4, pp. 64-69, 1960.
- [13] D. Lönard, R. Simon, V. Terzija, "Simulation von Netzmodellen mit zwei seitiger Einspeisung zum Test von Netzschutz-einrichtungen," TB-157/92, Univ. Kaiserslautern, 1992.

## 저 자 소 개



**Zoran Radojević**

He received B.S., M.S. and Ph.D. degrees in Electrical Engineering from the University of Belgrade. Currently, he is an Associate Professor in the Electrical Engineering Department at Konkuk University, Korea. He has been a Professor at Faculty of Electrical Engineering in Belgrade. He was also with Electrotechnology R&D Center, LG Industrial Systems Co., Ltd., Korea. His areas of research are power system protection, digital signal processing applications in power systems, short circuits, power system stability, high voltage engineering, power cables and electric power distribution systems. Dr. Radojević is Senior Member of the IEEE and a member of CIGRE.



**신 중 린 (慎 重 麟)**

1949년 9월 22일생. 1977년 서울대 공대 전기공학과 졸업. 1984년 동 대학원 전기공학과 졸업(석사). 1989년 동 대학원 전기공학과 졸업(공학박사). 현재 건국대학교 공과대학 전기공학과 교수.

Tel : 02-450-3487

E-mail : jrshin@konkuk.ac.kr